Applications and Applied Mathematics: An International Journal (AAM)

Volume 17 | Issue 2 Article 9

12-2022

(R1884) Motion of Variable Mass Body in the Seventh-Degree Henon-Heiles System

Shiv K. Sahdev
University of Delhi

Abdullah A. Ansari
International Center for Advanced Interdisciplinary Research (ICAIR)

Available at
http://pvamu.edu/aam
Appl. Appl. Math.
ISSN: 1932-9466

Applications and Applied Mathematics:
An International Journal
(AAM)

Vol. 17, Issue 2 (December 2022), pp. 439 – 449

Motion of Variable Mass Body in the Seventh-Degree Henon-Heiles System

[1]Shiv K. Sahdev and [1,2,*]Abdullah A. Ansari

[1]Department of Mathematics
Shivaji College, University of Delhi
Delhi, India
shiv_sahdev@yahoo.co.in

[2]International Center for Advanced Interdisciplinary Research (ICAIR)
Sangam Vihar, New Delhi, India
icairndin@gmail.com

*Corresponding author

Received: October 22, 2021; Accepted: December 21, 2021

Abstract

The goal of this paper is to reveal numerically the generalized Henon-Heiles system, that is, in the seventh-degree potential function where the smallest body mass varies. Utilizing the seventh degree potential function, we determine the equations of motion for the variable mass generalized Henon-Heiles system. Then we perform the graphical works such as locations of parking points, allowed regions of motion, and attracting domain basins. Lastly, using the Meshcherskii space transformations, we investigate stability states for these parking points.

Keywords: Henon-Heiles system; Variable mass; Seventh-degree; Stable; Unstable; Parking points; Regions

MSC 2010 No.: 70F15, 70F07

1. Introduction

Celestial mechanics is the part of applied mathematics and theoretical physics where one can study about the dynamical behavior of these celestial bodies. Either it is small or big as well as either

their shapes are point mass, spherical, oblate, triaxial, homogeneous, heterogeneous or with some other perturbations. To study the dynamical properties of these bodies, we should consider these bodies with a particular configuration. These configurations firstly started by Euler and then later many other researchers have investigated these problems with many configurations as restricted 3, 4, 5 and N body problems. Out of these problems, the restricted 3-body problem is the commonly studied problem with many special types of configurations such as: Copenhagen problem, Robes problem, Hills problem, Henon-Heiles problem, etc. One can see Bhatnagar et al. (1983), SubbaRao and Sharma (1997), Nagler (2004), Ishwar and Sharma (2012), Ansari (2018), Ansari (2020), Ansari (2021), Abouelmagd and Ansari (2021), Bouaziz and Ansari (2021), Sahdev and Ansari (2021) for details.

The classical case of Henon-Heiles problem was initially studied by Henon and Heiles (1964). This classical case problem contains the third-degree potential and from now onwards we will use CHHP for this problem in the paper. Now the generalization of CHHP is known as Generalized Henon-Heiles problem where it can have fifth or seventh-degree potential functions. This will be abbreviated as GHHP. GHHP is studied by some scientist as Zotos et al. (2018), Dubeibe et al. (2018), Dubeibe et al. (2020), and Llibre et al. (2021).

The losing or gaining of the mass of the celestial bodies are one of the attraction points for researchers, especially astronomers. Researchers such as Singh and Ishwar (1985), Lukyanov (2009), Zhang et al. (2012), Abouelmagd and Mostafa (2015), Ansari (2017), and Prasad and Ansari (2020) have investigated these configurations with variable mass of the celestial bodies.

The organization of the paper is as follows. An overview of the literature is given in the introduction section. The equations of motion and quasi-Jacobi integral are determined in Section 2. The graphical works (parking points, allowed regions of motion and attracting domain basins) are performed in Section 3 while the examination of stability of the parking points are presented in Section 4. The conclusion of the paper is given in Section 5.

2. Equations of motion

After fixing the dimension and using the procedure given by Dubeibe et al. (2020) and Abouelmagd and Ansari (2021), we can write the equations for the smallest body mass (m) motion when the mass variation originates from a single point and have negligible momenta as:

$$\begin{aligned} \ddot{x} + \frac{\dot{m}}{m}\,\dot{x} &= -\frac{\partial V_3}{\partial x}, \\ \ddot{y} + \frac{\dot{m}}{m}\,\dot{y} &= -\frac{\partial V_3}{\partial y}, \end{aligned} \tag{1}$$

where

$$\frac{\partial V_3}{\partial x} = V_{311} + \alpha\, V_{312}, \;\; \frac{\partial V_3}{\partial y} = V_{321} + \alpha\, V_{322},$$

$$V_3 = V_1 + \alpha\{x^6\,y + x^4\,y^3 + x^2\,y^5 + x^4\,y + x^2\,y^3 - \frac{y^5}{5} - \frac{y^7}{7} + \frac{1}{4}(x^2+y^2)^2 + \frac{1}{6}(x^2+y^2)^3\},$$

$$V_{311} = x(1+2\,y),\;\; V_{321} = x^2 + y(1-y),$$

$$V_{312} = 2\,x\,y(2x^2 + 3x^4 + y^2 + 2x^2\,y^2 + y^4) + x(x^2+y^2)(1+x^2+y^2),$$

$$V_{322} = x^2(1+x^2)(x^2+3\,y^2) + y^4(5x^2 - 1 - y^2) + y(x^2+y^2)(1+x^2+y^2).$$

By using Jeans law ($m = m_0\,e^{-t\,\delta_1}$) (Jeans (1928)) and Meshcherskii space transformations ($x = \delta_2^{-1/2}\xi,\; y = \delta_2^{-1/2}\,\eta$) (Meshcherskii (1949)), where δ_1 is a constant coefficient, $\delta_2 = \dfrac{m}{m_0}$ and m_0 is the initial mass, we can write the equations for the smallest variable mass body motion as:

$$\begin{aligned} \ddot{\xi} &= -\frac{\partial W}{\partial \xi}, \\ \ddot{\eta} &= -\frac{\partial W}{\partial \eta}, \end{aligned} \tag{2}$$

where

$$W = W_1 + \alpha\,W_2, \tag{3}$$

$$W_1 = \left(\frac{1}{2} - \frac{\delta_1^2}{8}\right)(\xi^2+\eta^2) + \delta_2^{-1/2}\left(\xi^2\,\eta - \frac{\eta^3}{3}\right),$$

$$W_2 = \delta_2^{-3/2}\left[\xi^4 + \eta + \xi^2\,\eta^3 - \frac{\eta^5}{5} + \delta_2^{-1}\left(\xi^6\,\eta + \xi^4\,\eta^3 + \xi^2\,\eta^5 - \frac{\eta^7}{7}\right)\right.$$
$$\left. + \frac{\delta_2^{1/2}}{4}(\xi^2+\eta^2)^2 + \frac{\delta_2^{-1/2}}{6}(\xi^2+\eta^2)^3\right].$$

The quasi-Jacobi integral from Equation (2) can be performed as:

$$\dot{\xi}^2 + \dot{\eta}^2 = 2\,W_1 + 2\,\alpha\,W_2 + E + 2\int_{t_0}^{t}\frac{\partial W_1}{\partial\,t}\,d\,t + 2\alpha\int_{t_0}^{t}\frac{\partial W_2}{\partial\,t}\,d\,t, \tag{4}$$

where E is the integral constant for our model. If we put $\alpha = 0$, then the equation for the quasi-Jacobi integral will reduce to the Jacobi integral for the classical Henon-Heiles system.

3. Graphical illustrations

The graphical works (parking points, allowed regions of motion, and attracting domain basins) are done numerically for this new model.

3.1. Parking points

By solving

$$\frac{\partial W}{\partial \xi} = 0 \quad \text{and} \quad \frac{\partial W}{\partial \eta} = 0,$$

numerically through the well-known software Mathematica, we get four parking points $L_{1,2,3,4}$, where L_1 lies on the positive side of the η-axis, L_2 lies at the origin, $L_{3,4}$ lie in the third and fourth quadrant respectively, both $L_{3,4}$ are symmetrical to each other about the η-axis, and are given in Figure (3). Figure 3(a) shows the constant mass case while Figures 3(b), 3(c), 3(d) show the variable mass cases. In Figures 3(a), 3(b), and 3(c), the color points are showing the location of parking points when the transition parameter α (= 0 (Black), 1 (Cyan), 5 (Blue) and 10 (Red)) varies. In these three cases, the locations of parking points $L_{1,2}$ are unchanged while the locations of parking points $L_{3,4}$ are changing and moving towards the η-axis as the vlaue of the transition parameter α, increases. In Figure 3(d), we fixed the value of transition parameter $\alpha = 4$ and increasing the value of the variation parameter δ_2 (0.4 (Black), 0.8 (Cyan), 1 (Blue) and 1.4 (Red)), we observed from that the location of parking point L_2 is unchanged while the location of the parking points $L_{1,3,4}$ are moving away. In this way, these parameters have an excellent effect on the locations of parking points.

3.2. Allowed regions of motion

The regions of motion are studied by evaluating the values of integral constant E corresponding to each parking points $L_{1,2,3,4}$ using the procedure given in Lukyanov (2009) and performed in Figure 2 as well as in Figure 3. Figure 2 shows the constant mass case while Figure 3 shows the variable mass case. In these figures, the cyan-colored regions represent the forbidden regions while white-colored regions represent the allowed regions for the motion. In part (a) of both figures, the parking point L_1 represents the smallest body that cannot move near the parking points $L_{2,3,4}$ while it can move near the parking point L_1 which works as a gateway for the allowed regions. In part (b) of both figures, the parking point L_2 represents the smallest body that can move near all four parking points $L_{1,2,3,4}$. In part (c) of both the figures, the parking point $L_{3,4}$ represents the smallest body that cannot move near the parking point L_2, while it can move near $L_{1,3,4}$. Moreover, the parking points $L_{3,4}$ works as a gateway for the allowed regions. The only difference between Figures 2 and 3 is that the allowed regions are shrinking in the variable mass case than the other case.

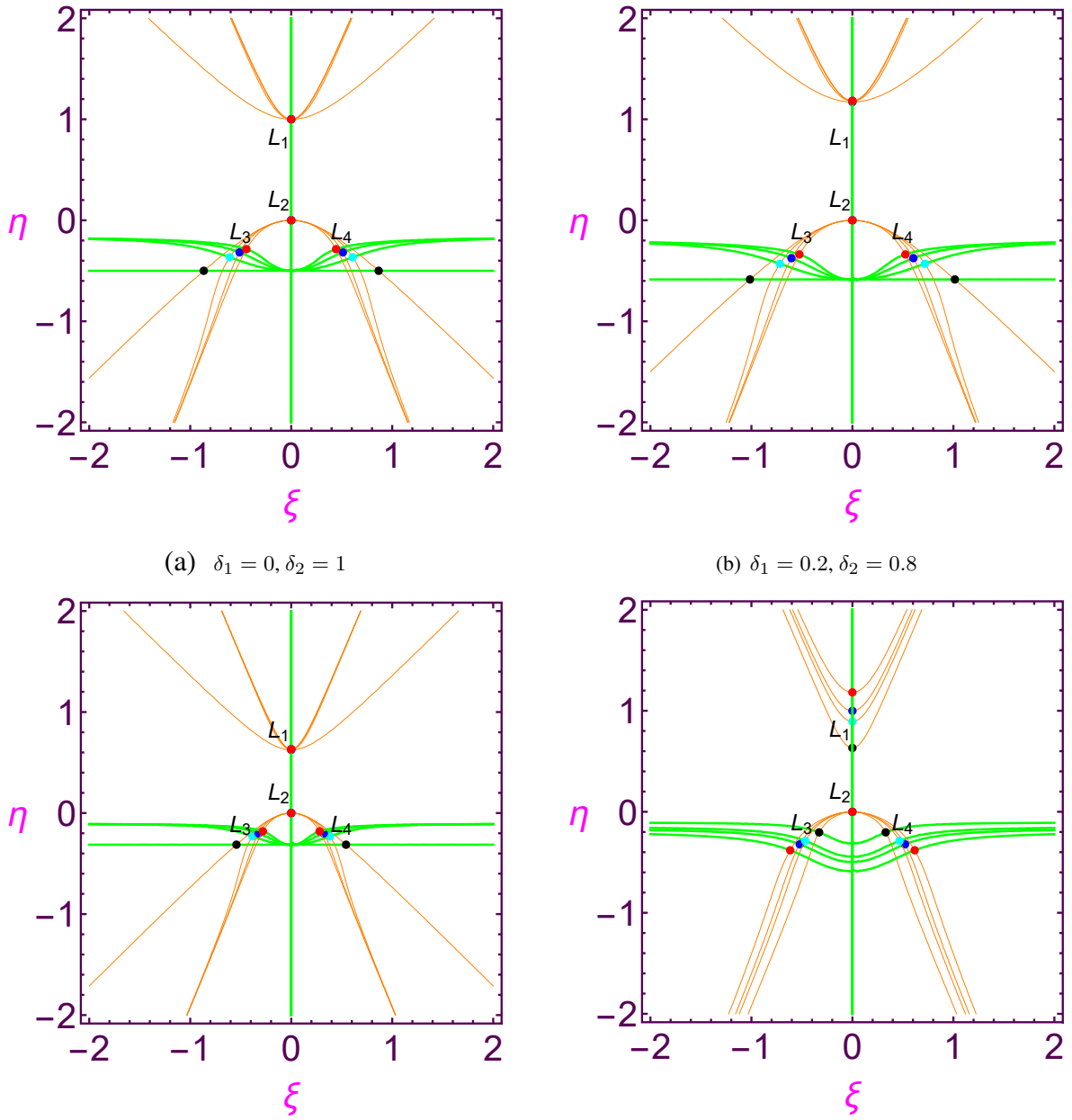

(a) $\delta_1 = 0, \delta_2 = 1$ (b) $\delta_1 = 0.2, \delta_2 = 0.8$

(c) $\delta_1 = 0.2, \delta_2 = 1.4$ (d) $\delta_1 = 0.2, \delta_2 = 0.4$ (Black), 0.8 (Cyan), 1 (Blue), 1.4 (Red)

Figure 1. Locations of parking points at α = 0 (Black), 1 (Cyan), 5 (Blue), 10 (Red)

3.3. Basins of attracting domain

Using the procedure given by Bouaziz and Ansari (2021), we have investigated the attractive dynamical properties, i.e., basins of attracting domain utilizing the Newton-Raphson method which is fast and simple than the other methods. The basins of attracting domain will appear when one of the initial points tends rapidly to one of the parking points, i.e., attracting points. We will use color code to explain the various attracting domains. We have investigated the attracting domain in constant mass case (Figures 4(a) and 4(b)) and variable mass case (Figures 4(c) and 4(d)) as well as

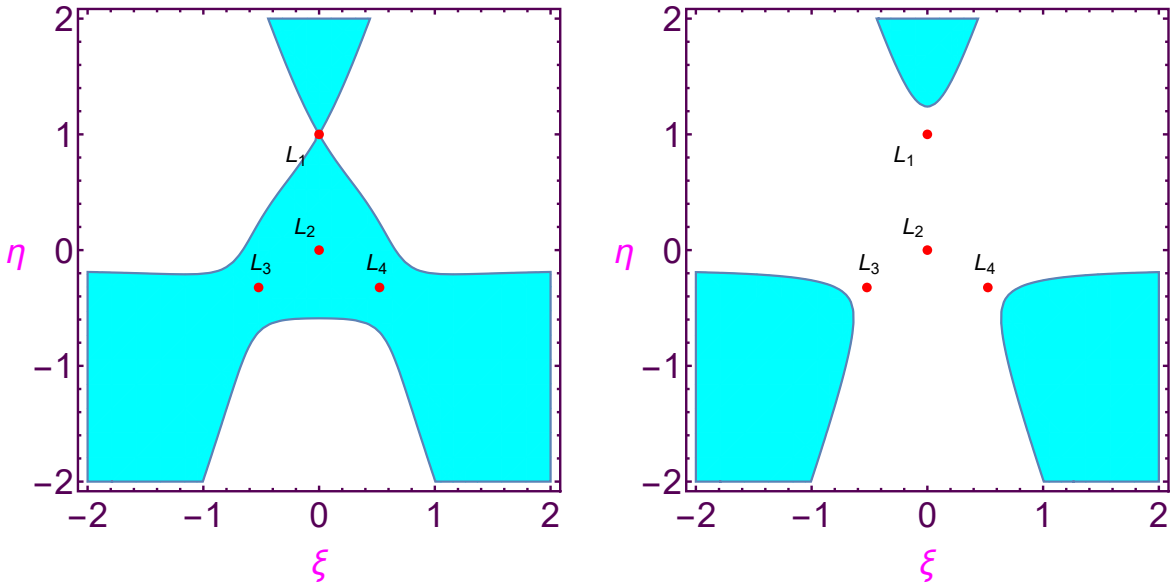

(a) Corresponding to L_1

(b) Corresponding to L_2

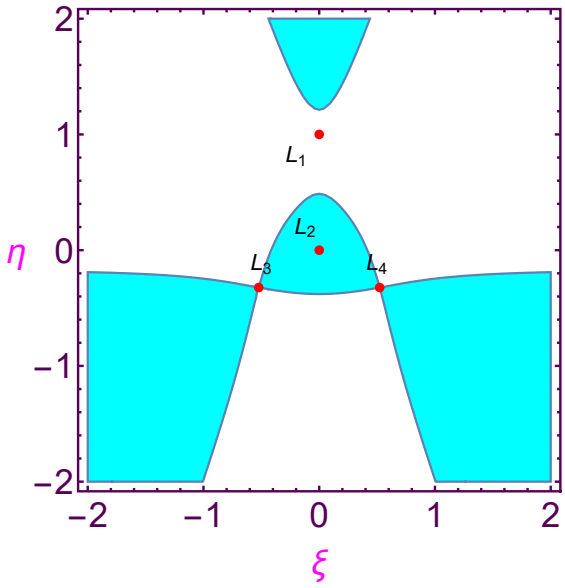

(c) Corresponding to $L_{3,4}$

Figure 2. Regions of motion with constant mass

shown the comparison between both cases. Figures 4(a) and 4(b) represent the CHHP and GHHP with constant mass, respectively, while Figures 4(c) and 4(d) represent the CHHP and GHHP with variable mass, respectively. In Figures 4(a) and 4(c), the attracting points L_1, L_2 and $L_{3,4}$ correspond to the red, cyan and light-yellow colored regions. These three colored regions extend to infinity. In Figures 4(b) and 4(d), the attracting points L_1, L_2 and $L_{3,4}$ correspond to the red, green and dark yellow colored regions. These three colored regions also extend to infinity. The main difference between these cases is that after introducing the variable mass in the model the regions are shrinking.

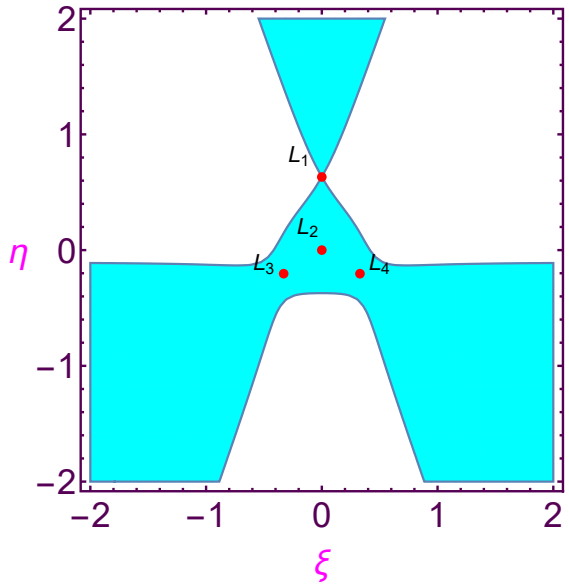

(a) Corresponding to L_1

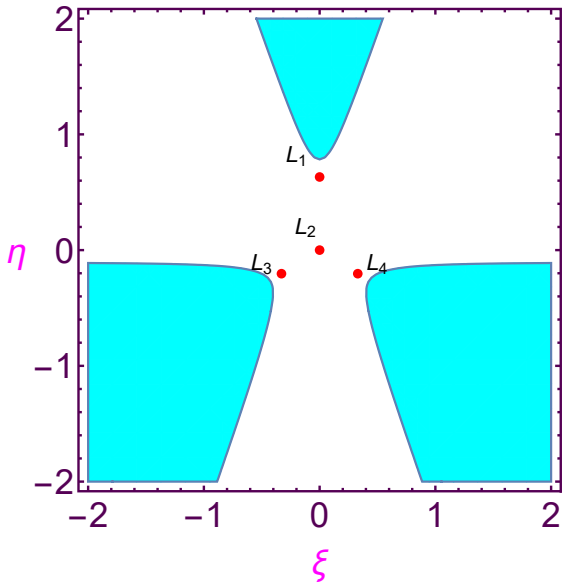

(b) Corresponding to L_2

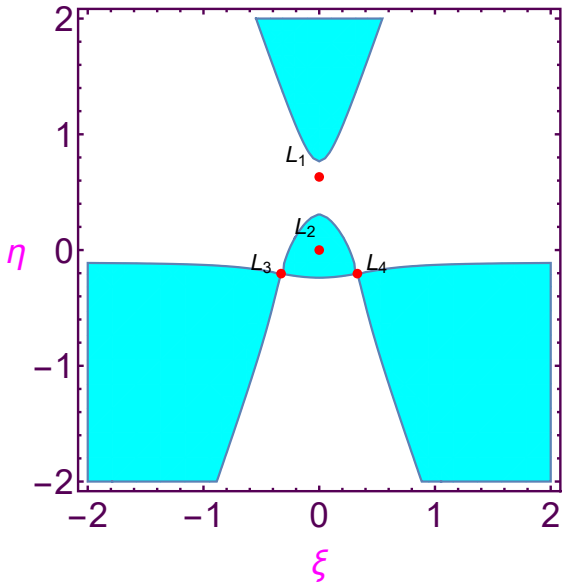

(c) Corresponding to $L_{3,4}$

Figure 3. Regions of motion with variable mass

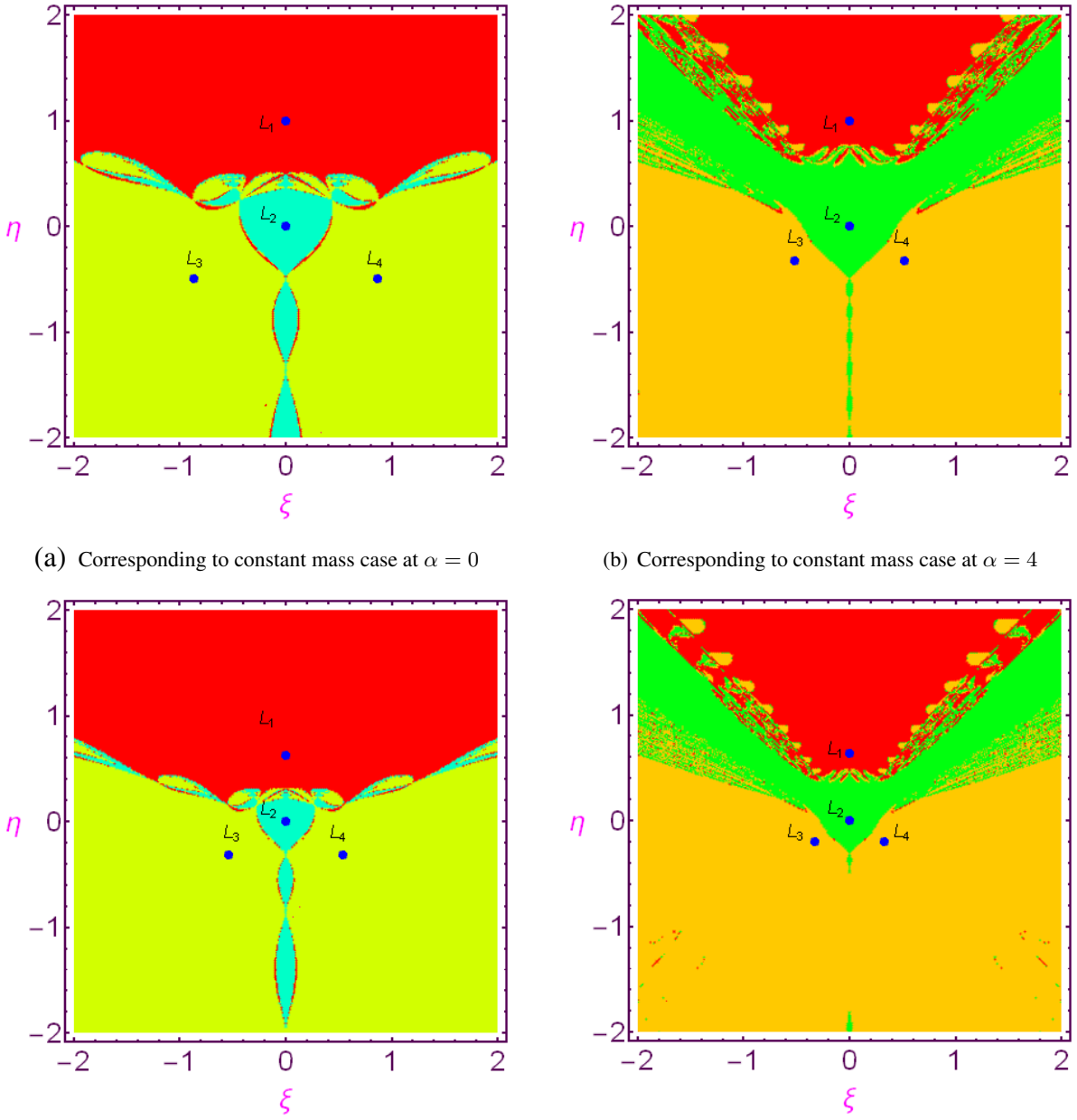

(a) Corresponding to constant mass case at $\alpha = 0$

(b) Corresponding to constant mass case at $\alpha = 4$

(c) Corresponding to variable mass case at $\alpha = 0$

(d) Corresponding to variable mass case at $\alpha = 4$

Figure 4. Basins of attracting domain for various cases

4. Instability

Following the methodology given by Abouelmagd and Ansari (2021) and using Meshcherskii space time inverse transformation, we can present the characteristic equation for our new model as

$$\lambda^4 + D_3\,\lambda^3 + D_2\,\lambda^2 + D_1\,\lambda + D_0 = 0, \tag{5}$$

$$D_3 = -2\,\delta_1,$$

$$D_2 = \frac{3}{2}\,\delta_1 + W^0_{\xi\xi} + W^0_{\eta\eta},$$

$$D_1 = -\frac{1}{2}\,\delta_1^3 - \,\delta_1(W^0_{\xi\xi} + W^0_{\eta\eta}),$$

$$D_0 = \frac{1}{16}\,\delta_1^4 + \frac{1}{4}\,\delta_1^2(W^0_{\xi\xi} + W^0_{\eta\eta}) + W^0_{\xi\xi}\,W^0_{\eta\eta} - (W^0_{\xi\eta})^2.$$

It is noticed that in the case of constant mass, the odd coefficients D_3 and D_1 will become zero and then the characteristic equation (8) will change to the quadratic equation in λ^2. The superscript 0 denotes the value of W at the corresponding parking point.

We solve the above characteristic equation (8) numerically corresponding to each parking points for the various values of the parameters used and get at least one positive real root or positive real part in all cases. Hence, all the parking points are unstable (see Table 1).

Table 1. Nature of Parking Points for Variable Mass Case at $\delta_1 = 0.2$, $\delta_2 = 0.4$ and $\alpha = 4$.

Parking points	Corresponding eigenroots	Nature
(0.0000000000, 0.0000000000)	$0.10000000005 \pm 0.9949874371\,i$ $0.10000000005 \pm 0.9949874371\,i$	Unstable
(0.0000000000, 0.6317507118)	-2.8894216612, 3.0894216612 $0.0999999999 \pm 5.1855439555\,i$	Unstable
$(-0.3296262907, -0.2037449029)$	-1.9376616369, 2.1376616369 $0.0999999999 \pm 2.2267413368\,i$	Unstable
$(0.3296262907, -0.2037449029)$	-1.9376616369, 2.1376616369 $0.0999999999 \pm 2.2267413368\,i$	Unstable

5. Conclusion

The GHHP is investigated by using the seventh-degree potential function. Using Jeans law and Meshcherskii space time transformation, we have determined the equations of motion and quasi-Jacobi integral where both are clearly depends on the parameters used, that is, variation parameters

as well as transition parameters. Afterwards, the graphical displays are constructed, such as locations of parking points, regions of possible motion and basins of attracting domain. Figures for parking points presented the locations of four parking points where we observed that as the values of the transition parameter and variation parameter increase, the locations of parking points are changing. Figures for the regions of motion illustrated the forbidden and allowed regions of motion in constant mass case and variable mass case, respectively. We observed in the variable mass case that the allowed regions are shrinking in respect to the other case. Figures for the basins of attracting domain performed in the constant mass case and variable mass case. We observed from here that the regions corresponding to the attracting points are extending to infinity. Also, in the variable mass case, attracting domains are shrinking in respect to the other case. Finally, the stability states of the parking points revealed that all the parking points are unstable. In this way, the parameters used have great influence on the motion of the smallest body.

Acknowledgment:

We are thankful to the editor and reviewers for their valuable comments to improve the manuscript at the present stage.

REFERENCES

Abouelmagd, E.I. and Mostafa, A. (2015). Out of plane equilibrium points locations and the forbidden movement regions in the restricted three-body problem with variable mass, Astrophys. Space Sci. doi:10.1007/s10509-015-2294-7

Abouelmagd, E.I. and Ansari, A.A. (2021). Variable mass motion in the Henon-Heiles system, Modern Physics Letters A, Vol. 36, No. 21. doi:10.1142/S0217732321501509

Ansari, A.A. (2017). Effect of Albedo on the motion of the infinitesimal body in circular restricted three-body problem with variable masses, Italian J. of Pure and Applied Math., Vol. 38, pp. 581–600.

Ansari, A.A. (2018). The circular restricted four- body problem with triaxial primaries and variable infinitesimal mass, Applications and Applied Mathematics: An International Journal, Vol. 13, No. 2, pp. 818-838.

Ansari, A.A. (2020). Behaviour of small variable mass particle in electromagnetic Copenhagen problem, Sultan Qaboos University Journal for Science, Vol. 25, No. 1, pp. 61-77.

Ansari, A.A. (2021). Heterogeneous primary in the restricted three-body problem with modified Newtonian potential of secondary, Bulgarian Astro. J., Vol. 35.

Bhatnagar, K.B. and Hallan, P.P. (1983). The effect of perturbation in the restricted problem of three bodies, Celest. Mech. Dyn. Astron., Vol. 30, pp. 97.

Bouaziz, F. and Ansari, A.A. (2021). Perturbed Hill's problem with variable mass, Astron. Nachr. doi:10.1002/asna.202113870

Dubeibe, F.L., Doncel, A.R. and Zotos, E.E. (2020). Dynamical analysis of bounded and unbounded orbits in a generalized Henon–Heiles system, Phys. Lett. A, Vol. 382, pp. 904–910.

Dubeibe, F.L., Zotos, E.E. and Chen, W. (2020). On the dynamics of a seventh-order generalized Hénon-Heiles potential, Results Phys, Vol. 18 (September), 103278.

Henon, M. and Heiles, C. (1964). The applicability of the third integral of motion: Some numerical experiments, Astron. J., Vol. 69, pp. 73–79.

Ishwar, B. and Sharma, J.P. (2012). Non-linear stability in photo-gravitational non-planer R3BP with oblate smaller primary, Astrophys. Space Sci., Vol. 337, pp. 563-571.

Jeans, J.H. (1928). Cambridge University Press, Cambridge.

Llibre, J., Saeed, T. and Zotos, E.E. (2021). Periodic orbits and equilibria for a seventh-order generalized Hénon-Heiles Hamiltonian system. J. of Geometry and Physics, Vol. 167, 1042901978

Lukyanov, L.G. (2009). On the restricted circular conservative three–body problem with variable masses, Astronomy Letters, Vol. 35, No. 5, pp. 349–359.

Meshcherskii, I.V. (1949). GITTL, Moscow.

Nagler, J. (2004). Crash test for Copenhagen problem, Phys. Rev. E, Vol. 69, 066218.

Prasad, S.N. and Ansari, A.A. (2020). Generalized elliptic restricted four-body problem with variable mass, Astron. Lett., Vol. 46, pp. 275–288.

Sahdev, S.K. and Ansari, A.A. (2021). Generalized Robe's problem having oblate heterogeneous primary containing viscous fluid inside the outer most layer and radiating spherical secondary with modified Newtonian potential, Sci. Int. Lahore, Vol. 33, No. 2, pp. 147-151.

Singh, J. and Ishwar, B. (1985). Effect of perturbations on the stability of triangular points in the restricted problem of three bodies with variable mass, Celest. Mech., Vol. 35, pp. 201–207.

SubbaRao, P.V. and Sharma, R.K. (1997). Effect of oblateness on the non-linear stability of L_4 in the restricted three-body problem, Celest. Mech. Dyn. Astron., Vol. 65, pp. 291–312.

Zhang, M.J., Zhao, C.Y. and Xiong, Y.Q. (2012). On the triangular libration points in photo-gravitational restricted 3-body problem with variable mass, Astrophys. Space Sci. doi:10.1007/s10509-011-0821-8

Zotos, E.E., Doncel, A.R. and Dubeibe, F.L. (2018). Basins of convergence of equilibrium points in the generalized Henon–Heiles system, Int. J. Non-Lin. Mech., Vol. 99, pp. 218–228.